Research article Available online www.ijsrr.org ISSN: 2279–0543

International Journal of Scientific Research and Reviews

Hall Current Effects on Peristaltic Transport of A Conducting Bingham Fluid With Permeable Walls By Adomian Decomposition Method

Laxmi Devindrappa * **and Naduvinamani N. B.**

Department of Studies and Research in Mathematics, Gulbarga University,
Kalaburagi-585106, Karnataka, India
E-mail**:** naduvinamaninb@yahoo.co.in , ldb.biradar@gmail.com

ABSTRACT

The influence of Hall current effect on peristaltic transport of a conducting Bingham fluid with permeable walls by Adomian decomposition method is examined. The non linear partial differential equations that govern that model were simplified under assumptions of long wavelength and low Reynolds number. This model is suitable for the blood flow in the sense that erythrocytes region and the plasma regions can be described as plug flow and non-plug flow regions. The velocity field for the model of interest is solved by Adomian decomposition method. The pressure gradient, pressure rise, stream functions and frictional force are discussed with the help of graphs drawn for different parameters like Darcy number, Hall parameter, Hartmann number and Slip parameter.

KEYWORDS: yield stress, frictional force, pressure gradient, pressure rise, stream functions and Adomian decomposition method.

NOMENCLATURE

b	:	Amplitude
c	:	Wave speed
F	:	Frictional force
m	:	Hall parameter
M	:	Hartmann number
Q	:	Time averaged flow rate
R_e	:	Reynolds number
λ	:	Wavelength
τ_{ij}	:	Stresses
τ_0	:	Yield stress.
α	:	Slip parameter
Δp	:	Pressure rise
D_a	:	Darcy number.

***Corresponding author**
Laxmi Devindrappa
Department of Studies and Research in Mathematics, Gulbarga University,
Kalaburagi-585106, Karnataka, India
E-mail**:** ldb.biradar@gmail.com

INTRODUCTION

Peristalsis is a series of wave-like muscle contractions that moves food to different processing stations in the digestive tract. The process of peristalsis begins in the esophagus when a bolus of food is swallowed. The strong wave-like motions of the smooth muscle in the esophagus carry the food to the stomach, where it is churned into a liquid mixture called chyme. Next, peristalsis continues in the small intestine where it mixes and shifts the chyme back and forth, allowing nutrients to be absorbed into the bloodstream through the small intestine walls. Peristalsis concludes in the large intestine where water from the undigested food material is absorbed into the bloodstream. Finally, the remaining waste products are excreted from the body. The mechanics of peristalsis has been examined by a number of investigators. Latham[1] was probably the first to investigate the mechanism of peristalsis in relation to mechanical pumping. Fung and Yih[2] presented a theoretical analysis of peristaltic transport primarily with inertia-free Newtonian flows driven by sinusoidal transverse waves of small amplitude. Investigation of peristaltic motion in connection with functions of different physiological systems such as the ureter, the gastro-intestinal tract, the small blood vessels and other glandular ducts was first made by Shapiro *et al.*[3].

The fluid mechanical description of the esophageal peristaltic transport with the help of two-fluid model has been explained by Brasseur[4]. Bugliarello and Sevilla[5] and Cockelet[6] have experimentally shown that blood has a peripheral layer of plasma and a core region of suspension of all the erythrocytes when it flows through small blood vessels. Srivastava and Srivastava[7] have investigated the problem of peristaltic transport of blood in a uniform and non-uniform geometries by considering blood as a two layered fluid model consisting of a central layer of suspension of all erythrocytes, etc assumed to be a Casson fluid, which is a yield stress fluid and a peripheral layer of plasma as a Newtonian fluid. Comparani and Mannucci[8] have analyzed the flow of a Bingham fluid in contact with a Newtonian fluid in a channel. Electro-Kinetically driven peristaltic transport of viscoelastic physiological fluids through a finite length capillary analysed by Tripathi *et al.*[9] . Vajravelu *et al.*[10] studied the peristaltic pumping of a Casson fluid in an elastic tube. Rathod and Laxmi[11] have studied the effects of heat transfer on the peristaltic MHD flow of a Bingham fluid through a porous medium in a channel.

If a particle is at rest in presence of magnetic field, the field has no effect. Similarly, if the particle path is in the same direction as that of the magnetic field, there is no effect i.e. the particle motion will be undeflected. But if the particle path has a component normal to the direction of magnetic field, the particle will be deflected. In presence of magnetic field of large extent at right

angle to the direction of motion of a charged particle, the particle is deflected in a circular path. In addition to this deflection the particle experiences the electric field. The combined force acting on the particle is said to be Lorentz force. Conductivity normal to the magnetic field is reduced due to the free spiraling of electrons and ions about the magnetic lines of force before suffering collisions and a current is induced in direction normal to both the electric and magnetic fields. This phenomenon is called the Hall Effect. When the magnetic field is very strong the Hall Effect cannot be neglected. Hayat *et al.*[12] have investigated the peristaltic flow of a Maxwell fluid including the Hall Effect through porous medium. Asghar *et al.*[13] studied the effects of Hall current and heat transfer on flow due to a pull of eccentric rotating disk. The effect of Hall currents on interaction of pulsatile and peristaltic transport induced flows of a particle fluid suspension that had been examined by Gad[14]. Hussain *et al.*[15] studied the Heat and mass transfer analysis in variabl eviscosity peristaltic flow with Hall current and ion slip. Ellahi *et al.*[16] examined theoretically the peristaltic flow of Jeffrey fluid in a non-uniform rectangular duct under the effects of Hall and ion slip. Hall effects on peristalsis of boron nitride-ethylene glycol nanofluid with temperature dependent thermal conductivity investigated by Abbasi *et al.*[17].

With the above discussion in mind, the purpose of the present investigation is to analyse the Hall current effects on peristaltic transport of a conducting Bingham fluid with permeable walls by Adomian decomposition method under the assumptions of long wavelength and low Reynolds number. The expressions for the velocity field and pressure gradient are obtained analytically. The impact of all the physical parameters of interest is taken into consideration with the help of graphs.

MATHEMATICAL FORMULATION

Consider the peristaltic pumping of a conducting Bingham fluid in a channel with permeable walls, under long wavelength and low Reynolds number assumptions. A longitudinal train of progressive sinusoidal waves takes place on the upper and lower walls of the channel. We assume that a uniform magnetic field strength B_0 is applied. For simplicity, we restrict our discussion to the half-width of the channel as shown in the figure.1. The region between $y=0$ and $y=y_0$ is called plug flow region. In the plug flow region $|\tau_{yx}| \le \tau_0$. In the region between $y=y_0$ and $y=H$, $|\tau_{yx}| > \tau_0$. The wall deformation is given by

$$H(X,t) = a + b\sin\frac{2\pi}{\lambda}(\bar{x} - c\bar{t}) \qquad (1)$$

where b is the amplitude, λ the wavelength and c is the wave speed. Under the assumptions that the channel length is an integral multiple of the wavelength λ and the pressure difference across

the ends of the channel is a constant, the flow becomes steady in the wave frame $(\bar{x},\bar{y})$ moving with velocity c away from the fixed (laboratory) frame $(\bar{X},\bar{Y})$ .The transformation between these two frames is given by

$$\bar{x}=\bar{X}-ct,\bar{y}=\bar{Y},\bar{u}(x,y)=\bar{U}(X-ct,Y)and\ \bar{w}(x,y)=\bar{W}(X-ct,Y) \quad (2)$$

Where $\bar{U}$ and $\bar{W}$ are velocity components in the laboratory frame and $\bar{u}$ and $\bar{w}$ are velocity components in the wave frame. In the many physiological situations it is proved experimentally that the Reynolds number of the flow is very small. So, we assume that the wavelength is infinite. So the flow is of Poiseuille type at each local cross - section.

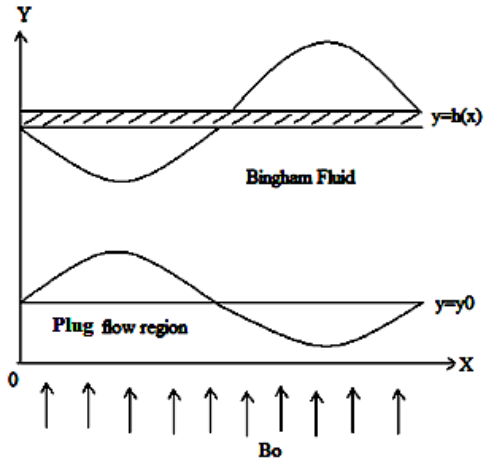

Fig. 1. The Physical model

The equations governing the flow in wave frame are given by

$$\frac{\partial\bar{u}}{\partial\bar{x}}+\frac{\partial\bar{w}}{\partial\bar{y}}=0. \quad (3)$$

$$\rho\left(\frac{\partial\bar{u}}{\partial\bar{t}}+\bar{u}\frac{\partial\bar{u}}{\partial\bar{x}}+\bar{w}\frac{\partial\bar{u}}{\partial\bar{y}}\right)=-\frac{\partial\bar{p}}{\partial\bar{x}}+\frac{\partial\bar{\tau}_{\bar{x}\bar{x}}}{\partial\bar{x}}+\frac{\partial\bar{\tau}_{\bar{y}\bar{x}}}{\partial\bar{y}}+\frac{\sigma B_0^{\,2}}{1+m^2}(-(\bar{u}+c)+m\bar{w}). \quad (4)$$

$$\rho\left(\frac{\partial\bar{w}}{\partial\bar{t}}+\bar{u}\frac{\partial\bar{w}}{\partial\bar{x}}+\bar{w}\frac{\partial\bar{w}}{\partial\bar{y}}\right)=-\frac{\partial\bar{p}}{\partial\bar{y}}+\frac{\partial\bar{\tau}_{\bar{x}\bar{y}}}{\partial\bar{x}}+\frac{\partial\bar{\tau}_{\bar{y}\bar{y}}}{\partial\bar{y}}-\frac{\sigma B_0^{\,2}}{1+m^2}(\bar{w}+m(\bar{u}+c)). \quad (5)$$

Where $m=\frac{\sigma B_0}{en}$ is the hall parameter, e-Electron charge, n-number density of electrons and τ_{ij} denote the stresses. For the Bingham plastic these are strains through the constitutive model,

$$\tau_{ij}=\left(\mu+\frac{\tau_y}{\dot{\gamma}}\right)\dot{\gamma}_{ij} \quad \text{for} \quad \tau\geq\tau_0 \text{ and,} \quad (6)$$

$$\tau_{ij}=\dot{\gamma}_{ij}=0 \qquad \text{for} \qquad \tau<\tau_0. \quad (7)$$

Where $\dot{\gamma}_{ij}$ is the rate of strain tensor,

$$\dot{\gamma}_{ij} = \frac{\partial u_i}{\partial x_j} + \frac{\partial u_j}{\partial x_i}, \tag{8}$$

$$\tau = \sqrt{\frac{1}{2}\tau_{ij}\tau_{ij}} \quad \text{and} \quad \dot{\gamma} = \sqrt{\frac{1}{2}\dot{\gamma}_{ij}\dot{\gamma}_{ij}} = \sqrt{\left(\frac{\partial u}{\partial x}\right)^2 + \left(\frac{\partial w}{\partial y}\right)^2 + \left(\frac{\partial u}{\partial y} + \frac{\partial w}{\partial x}\right)^2}. \tag{9}$$

$$\tau_{xy} = \frac{\partial u}{\partial y} - \tau_0 \quad \text{for} \quad \tau \geq \tau_0 \ ,$$

$$\tau_{xy} = 0 \quad \text{for} \quad \tau < \tau_0 .$$

Introducing the non-dimensional quantities

$$x = \frac{\bar{x}}{\lambda}, y = \frac{\bar{y}}{a}, u = \frac{\bar{u}}{c}, w = \frac{\bar{w}}{c\delta}, p = \frac{\bar{p}a^2}{\mu c\lambda}, t = \frac{c\bar{t}}{\lambda}, h = \frac{H}{a}, \phi = \frac{b}{a}, \tau_0 = \frac{a\bar{\tau}_0}{\lambda}, y_0 = \frac{\bar{y}_0}{a},$$

$$M = \sqrt{\frac{\sigma}{\mu}}aB_0, \ \mathrm{Re} = \frac{\rho ca}{\mu}, Da = \frac{k}{a^2}, \ \tau_{xx} = \frac{\lambda}{\mu c}\bar{\tau}_{\bar{x}\bar{x}}, \ \tau_{xy} = \frac{a}{\mu c}\bar{\tau}_{\bar{x}\bar{y}}, \ \tau_{yy} = \frac{a}{\mu c}\bar{\tau}_{\bar{y}\bar{y}}$$

Into equations (3) to (5), we get (dropping the bars)

$$\frac{\partial u}{\partial x} + \frac{\partial w}{\partial y} = 0 \tag{10}$$

$$\mathrm{Re}\delta\left(u\frac{\partial u}{\partial x} + w\frac{\partial u}{\partial y}\right) = -\frac{\partial p}{\partial x} + \delta^2\frac{\partial \tau_{xx}}{\partial x} + \frac{\partial \tau_{yx}}{\partial y} - \frac{M^2}{1+m^2}(u + 1 + m\delta w) \tag{11}$$

$$\mathrm{Re}\delta^3\left(u\frac{\partial w}{\partial x} + w\frac{\partial w}{\partial y}\right) = -\frac{\partial p}{\partial y} + \delta^2\frac{\partial \tau_{xy}}{\partial x} + \delta\frac{\partial \tau_{yy}}{\partial y} - \frac{M^2}{1+m^2}\left(w\delta + m(u+1)\right) \tag{12}$$

where

$$\tau_{ij} = \left(\mu + \frac{\tau_0}{\dot{\gamma}}\right)\dot{\gamma}_{ij} \quad \text{for} \quad \tau \geq \tau_0 \tag{13}$$

$$\tau_{ij} = \dot{\gamma}_{ij} = 0 \quad \text{for} \quad \tau < \tau_0 \tag{14}$$

$$\dot{\gamma}_{xy} = \dot{\gamma}_{yx} = \frac{\partial u}{\partial y} + \delta^2\frac{\partial u}{\partial x} \tag{15}$$

$$\dot{\gamma}_{xx} = 2\delta\frac{\partial u}{\partial x}, \quad \dot{\gamma}_{yy} = 2\delta\frac{\partial w}{\partial y} \tag{16}$$

$$\dot{\gamma} = \sqrt{2\delta^2\left(\left(\frac{\partial u}{\partial x}\right)^2 + \left(\frac{\partial w}{\partial y}\right)^2\right) + \left(\frac{\partial u}{\partial y} + \delta^2\frac{\partial w}{\partial x}\right)^2} \tag{17}$$

$$\tau = \sqrt{\tau^2_{xy} + \delta^2 \tau^2_{xx}} \tag{18}$$

Under the assumptions of long wavelength and low Reynolds number, the equations (11) to (12) reduce to

$$0 = -\frac{\partial p}{\partial x} + \frac{\partial \tau_{yx}}{\partial y} - \frac{M^2}{1+m^2}(u+1) \tag{19}$$

$$0 = -\frac{\partial p}{\partial y} \tag{20}$$

$$\tau_{xy} = \frac{\partial u}{\partial y} - \tau_0 \quad \text{for} \quad \tau \geq \tau_0 \tag{21}$$

$$\tau_{xy} = 0 \quad \text{for} \quad \tau < \tau_0 \tag{22}$$

Here τ_0 is the yield stress.

Here equation (20) indicates that p is independent of y and depends only upon x. Therefore, Eq. (19), can be rewritten as

$$\frac{\partial^2 u}{\partial y^2} = \frac{dp}{dx} + \frac{M^2}{1+m^2}(u+1) \tag{23}$$

The non-dimensional boundary conditions are

$$\frac{\partial u}{\partial y} = \tau_0 \text{ at } y = 0 \tag{24}$$

$$u = -1 - \frac{\sqrt{Da}}{\alpha}\frac{\partial u}{\partial y} \text{ at } y = h \tag{25}$$

Where α is slip parameter and τ_0 is the yield stress.

The volume flux q through each cross section in the wave frame is given by

$$q = \int_0^{y_0} u_p dy + \int_{y_0}^{h} u dy \tag{26}$$

The instantaneous volume flow rate $Q(X,t)$ in the laboratory frame between the centre line and the wall is

$$Q(X,t) = \int_0^H U dy = \int_0^h (u+1) dy = q + h \tag{27}$$

SOLUTION OF THE PROBLEM

For the solution of Eq. (23), we use Adomian decomposition method, we write Eq. (23) in operator form

$$L_{yy}u = \frac{M^2}{1+m^2}(u) + \frac{dp}{dx} + \frac{M^2}{1+m^2} \tag{28}$$

Where $L = \frac{\partial^2}{\partial y^2}$ Since L is a second-order differential operator, L^{-1} is a second-fold integration operator defined by:

$$L^{-1}(.) = \int_0^y \int_0^y (.)\,dy\,dy\,. \tag{29}$$

Operating with L^{-1}, Eq. (28) becomes

$$u = c_1 + c_2 y + L^{-1}\left(\frac{dp}{dx} + \frac{M^2}{1+m^2}\right) + L^{-1}\left(\frac{M^2}{1+m^2}(u)\right) \tag{30}$$

In which the function can be determined by utilizing the boundary conditions (24-25). By the standard Adomian decomposition method, one can write:

$$u = \sum_{n=0}^{\infty} u_n$$

From eq. (30)

$$u_0 = c_1 + c_2 y + \left(\frac{dp}{dx} + \frac{M^2}{1+m^2}\right)\frac{y^2}{2!} \tag{31}$$

$$u_{n+1} = \frac{M^2}{1+m^2} L^{-1}(u_n), \qquad n \geq 0\,. \tag{32}$$

from (31) and (32), we obtain

$$u_1 = c_1 \frac{(Ny)^2}{2!} + \frac{c_2}{N}\frac{(Ny)^3}{3!} + \left(\frac{dp}{dx} + N^2\right)\frac{1}{N^2}\frac{(Ny)^4}{4!} \tag{33}$$

$$u_2 = c_1 \frac{(Ny)^4}{4!} + \frac{c_2}{N}\frac{(Ny)^5}{5!} + \left(\frac{dp}{dx} + N^2\right)\frac{1}{N^2}\frac{(Ny)^6}{6!} \tag{34}$$

$$u_n = c_1 \frac{(Ny)^{2n-2}}{2n!} + \frac{c_2}{N}\frac{(Ny)^{2n-1}}{(2n-1)!} + \left(\frac{dp}{dx} + N^2\right)\frac{1}{N^2}\frac{(Ny)^{2n}}{(2n)!} \tag{35}$$

using equations (31, 33, 34 and 35) in Eq. (32) we get

$$u = c_1 \cosh(Ny) + \frac{c_2}{N}\sinh(Ny) + \left(\frac{dp}{dx} + N^2\right)\frac{1}{N^2}\left(\cosh(Ny) - 1\right) \quad . \tag{36}$$

where $N = \frac{M^2}{1+m^2}$ and subject to the boundary conditions (24) and (25) we obtain

$$c_2 = \tau_0 \ , \tag{37}$$

$$c_1 = \frac{1}{\left(\cosh[Nh] + \frac{\sqrt{Da}}{\alpha} N \sinh[Ny]\right)} \begin{pmatrix} -1 - \frac{\sqrt{Da}}{\alpha}\left(\tau_0 \cosh[Ny] + \left(\frac{dp}{dx} + N^2\right)\frac{1}{N}\sinh[Ny]\right) \\ -\frac{\tau_0}{N}\sinh[Nh] - \left(\frac{dp}{dx} + N^2\right)\frac{1}{N^2}\left(\cosh[Nh] - 1\right) \end{pmatrix} \tag{38}$$

From equations (36, 37 and 38) we obtain

$$u = -\frac{\frac{dp}{dx}\left(1 - \frac{\alpha\, Cosh[h\,y]}{\alpha\, Cosh[h\,N] + \sqrt{Da}\, N\, Sinh[N\,y]}\right)}{N^2} - \frac{N^2 + \frac{N\,\tau_y\left(\sqrt{Da}\, N + \alpha\, Sinh[N\,(h-y)]\right)}{\alpha\, Cosh[h\,N] + \sqrt{Da}\, N\, Sinh[N\,y]}}{N^2} \tag{39}$$

Taking in equation (39) $y = y_0$, we get the velocity in the plug flow region as u_p

$$u_p = -\frac{\frac{dp}{dx}\left(1 - \frac{\alpha\, Cosh[h\,y_0]}{\alpha\, Cosh[h\,N] + \sqrt{Da}\, N\, Sinh[N\,y_0]}\right)}{N^2} - \frac{N^2 + \frac{N\,\tau_y\left(\sqrt{Da}\, N + \alpha\, Sinh[N\,(h-y_0)]\right)}{\alpha\, Cosh[h\,N] + \sqrt{Da}\, N\, Sinh[N\,y_0]}}{N^2}$$

The volume flux q through each cross section in the wave frame is given by

$$q = \int_0^{y_0} u_p\, dy + \int_{y_0}^{h} u\, dy = -h + A_1 A_2 - A_3 - A_4 + y_0 - A_5 + \frac{dp}{dx}\left(A_6 - A_7\right) \tag{40}$$

Where $A_1 = \frac{1}{\sqrt{Da}\, N^3}\sqrt{2}\,\tau_0\, Tan^{-1}\left[\frac{\sqrt{2}\left(\sqrt{Da}\, N - \alpha Cosh[hN] Tan[\frac{1}{2}N(h-y_0)]\right)}{\sqrt{-2Da\,N^2 - \alpha^2 - \alpha^2 Cosh[2hN]}}\right]$.

$$A_2 = \sqrt{-2Da\,N^2 - \alpha^2 - \alpha^2 Cosh[2hN]}$$

$$A_3 = \frac{\alpha\,\tau\, Log[\alpha\, Cosh[hN] + \sqrt{Da}\, N\, Sinh[N(h-y_0)]]\, Sinh[hN]}{\sqrt{Da}\, N^3}$$

$$A_4 = \frac{N^2 + \frac{N\,\tau_0\left(\sqrt{Da}\, N + \alpha\, Sinh[N(h-y_0)]\right)}{\alpha\, Cosh[hN] + \sqrt{Da}\, N\, Sinh[hy_0]}}{N^2}$$

$$A_5 = \frac{\alpha\,\tau_0 Cosh[hN]\left(-h + y_0\right)}{\sqrt{Da}\, N^2}$$

$$A_6 = \frac{\alpha\, Log[\alpha\, Cosh[hN] + \sqrt{Da}\, N\, Sinh[N(h-y_0)]]}{\sqrt{Da}\, N^4}$$

$$A_7 = \frac{1 - \frac{\alpha\, Cosh[Ny_0]}{\alpha\, Cosh[hN] + \sqrt{Da}\, N\, Sinh[hy_0]}}{N^2} + \frac{-h + y_0}{N^2}$$

From Eq. (40) we have

$$\frac{dp}{dx} = \frac{\left(q - \left(-h + A_1 A_2 - A_3 - A_4 + y_0 - A_5\right)\right)}{\left(A_6 - A_7\right)} \tag{41}$$

The pressure rise and frictional force over one wavelength of the peristaltic are given by

$$\Delta p = \int_0^1 \frac{dp}{dx} dx \tag{42}$$

$$F = \int_0^1 h\left(-\frac{dp}{dx}\right) dx \tag{43}$$

The above integrals numerically evaluated using the MATHEMATICA software.

RESULTS AND DISCUSSION

We have presented a set of Figures 2-16, which describe qualitatively the effects of various parameters of interest on flow quantities such as pressure gradient, pressure rise per wavelength, frictional force and stream functions.

Figures 2-5 show the variations of the axial pressure gradient $\frac{dp}{dx}$ with respect to the axial x which has oscillatory behavior in the whole range of the x-axis for all other parameters, Figure 2 depicts the impact of Hall parameter m on axial pressure gradient. It shows that axial pressure gradient decreases in the channel. Influence of magnetic field parameter M on pressure gradient depicted in figure 3. Indeed, the axial pressure gradient increases by increase in M. In Figure 4, It can be notice that the axial pressure gradient reduces by increase in Da. Figure 5 depicts that $\frac{dp}{dx}$ is increases with the increases of α.

The pressure rise per wavelength Δp against flow rate for different values Hall parameter m, Darcy number D_a, Hartmann number M and slip parameter α, can be observed from Figs.6-9. It is observed from the Fig.6, that, in the pumping region the pumping rate decreases by increasing Hall parameter m, while in the co-pumping region the pumping rate increases by increasing Hall parameter m, For the free pumping case there are no noticeable difference observed . The variation of pressure rise with time averaged flow rate Q for different values of magnetic parameters M is shown in Fig. 7, it is observed that the larger the magnetic parameter greater the pressure rise against which the pump works. For free pumping the flux Q depends on magnetic field and it increases with

increasing magnetic parameter M. The variation of pressure rise with time averaged flow rate Q for different values of Da is shown in Fig. 8, for a given pressure rise the flux Q depends on Darcy number and it decreases with increasing Darcy number Da. For free pumping the flux Q is constant and it is independent of Da. The variation of pressure rise with time averaged flow rate Q for different values of α is shown in Fig.9, it is observed that the longer the slip parameter, the greater the pressure rise against which the pump works. For a given flux Q, the pressure difference Δp increases with increasing slip parameter. From Figs. 10-13 it can be seen that frictional forces have opposite behavior as compared to the pressure rise. Formation of circular bolus by internally splitting of streamlines is known as trapping. The bolus moves forward through peristaltic wave with the same speed. Figure 14 indicate that for ascending values of Hall parameter m, the size of trapped bolus becomes larger. Figure 15 indicate indicate that for large value of Hartman number M the size of trapped bolus increases. Figure 13 depicts that increasing Q led to an increase in trapped bolus size

CONCLUSION

This paper has presented the mathematical model that describes Hall current effects on peristaltic transport of a conducting Bingham fluid with permeable walls by Adomian decomposition method. The governing two dimensional equations have been simplified under the assumptions of low Reynolds number and long wavelength. The simplified equations are solved analytically using Adomian decomposition method. A set of graphs were plotted in order to analyze the effects of various physical parameters on these solutions. Key findings of present analysis are summarized below.

- It is observed that pressure gradient decreases with the increase of m and Da while it increases by increasing M and α.
- It is observed that pressure rise decreases with the increase in Da and m. However it increases with an increase in M and α.
- Hartman number and Hall parameter have opposite effects on pressure gradient and pressure rise per wavelength.
- It is observed that the friction force has an opposite character in comparison to the pressure rise.
- Trapped bolus size enhances with increase in the Hall parameter m, Hartman number M.

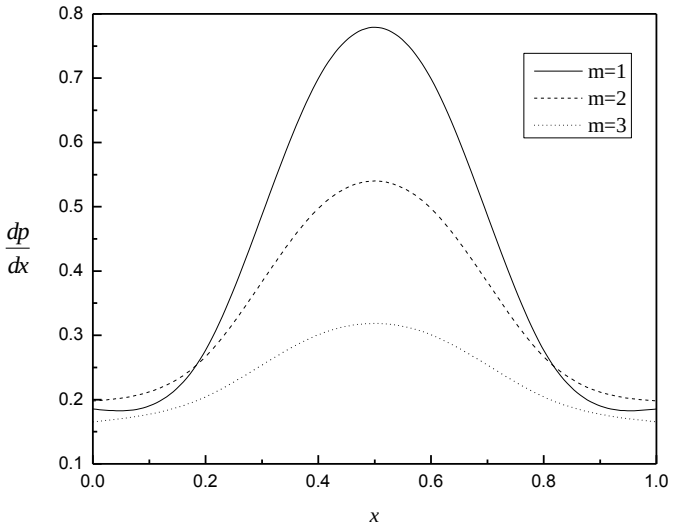

Fig. 2. The variation of pressure rise with time-averaged flux for different values m for

$$\varphi = 0.6,\ Da = 0.01,\ \alpha = 0.1,\ M = 2,\ y_0 = 0.2 \text{ and } \tau = 0.01$$

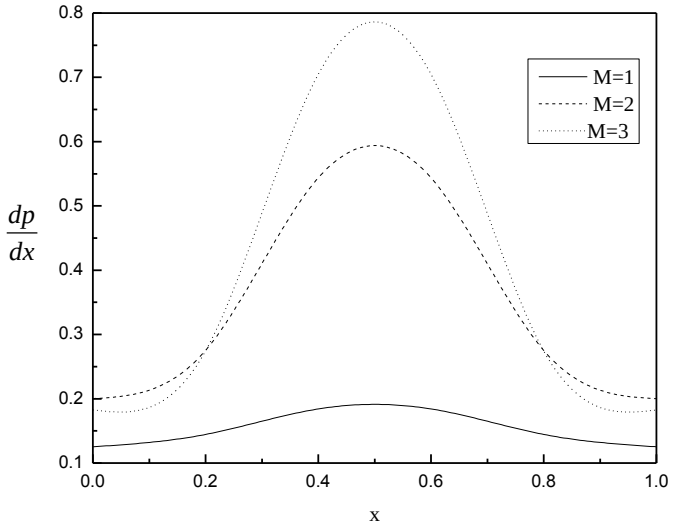

Fig. 3. The variation of axial pressure gradient with M for

$$\varphi = 0.6,\ Da = 0.01,\ \alpha = 0.1,\ m = 2,\ y_0 = 0.2 \text{ and } \tau = 0.1$$

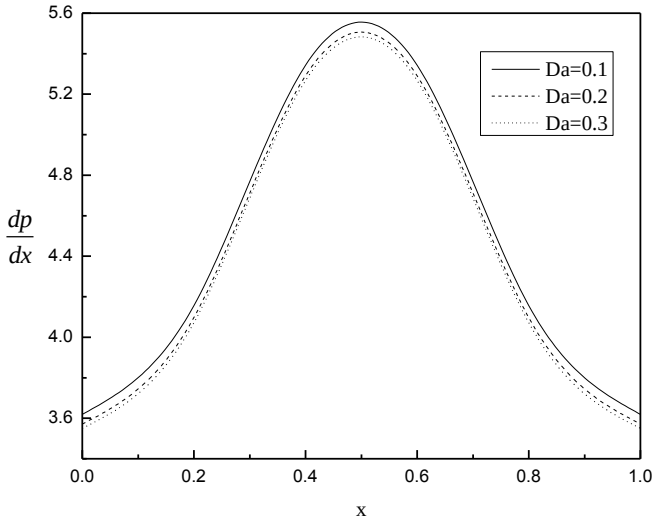

Fig.4. The variation of axial pressure gradient with Da for

$\varphi = 0.6,\ M = 4,\ \alpha = 0.1,\ m = 1,\ y_0 = 0.2$ and $\tau = 0.01$

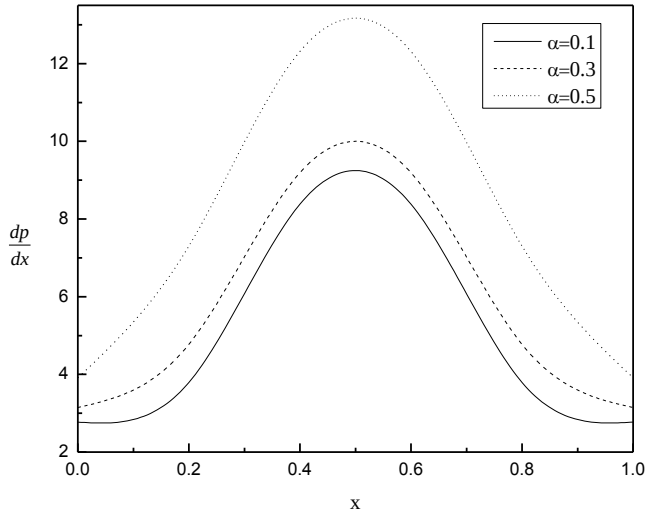

Fig.5. The variation of axial pressure gradient with α for

$\varphi = 0.6,\ M = 2,\ Da = 0.01,\ m = 1,\ y_0 = 0.2$ and $\tau = 0.01$

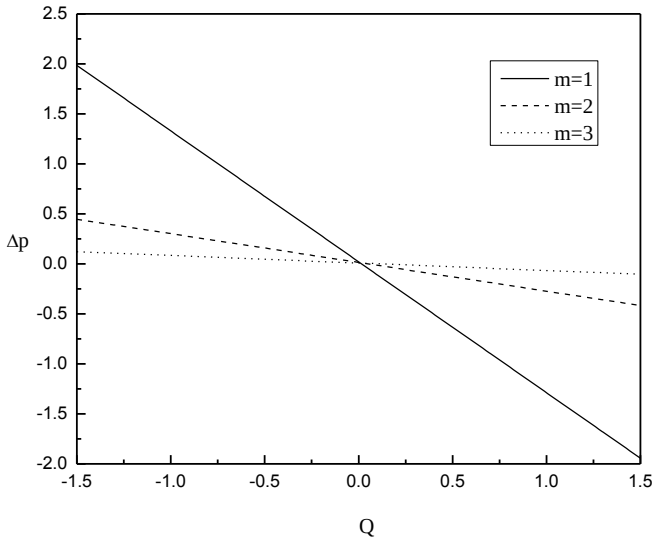

Fig. 6. The variation of pressure rise with time-averaged flux for different values m for

$$\varphi = 0.6,\ Da = 0.01,\ \alpha = 0.1,\ M = 2,\ y_0 = 0.2 \text{ and } \tau = 0.01$$

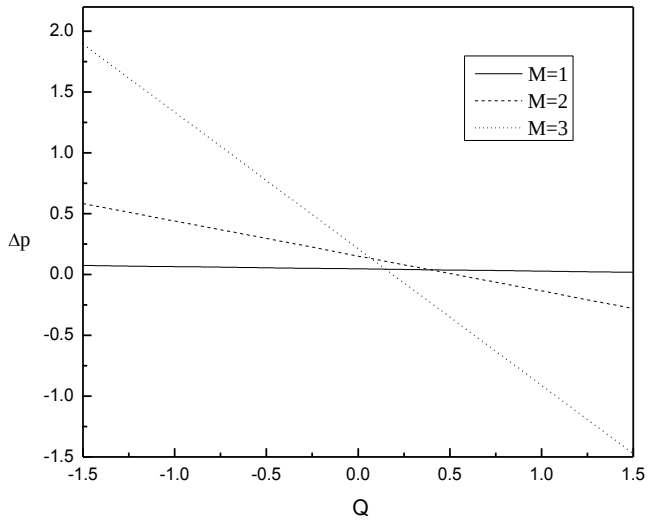

Fig. 10. The variation of pressure rise with time-averaged flux for different values M for

$$\varphi = 0.6,\ Da = 0.01,\ \alpha = 0.1,\ m = 2,\ y_0 = 0.2 \text{ and } \tau = 0.1$$

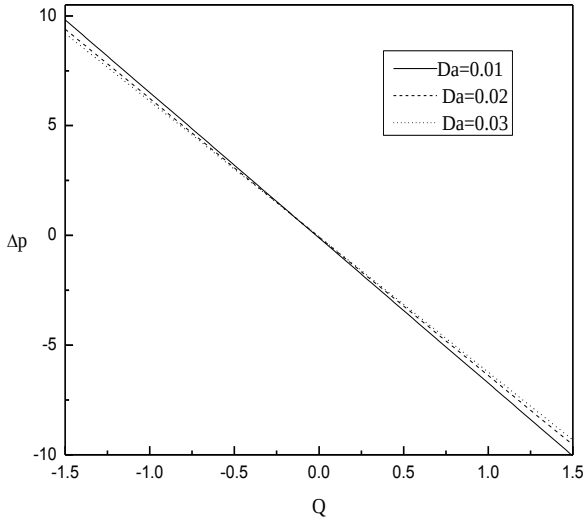

Fig.8. The variation of pressure rise with time-averaged flux for different values Da for

$\varphi = 0.6,\ M = 4,\ \alpha = 0.1,\ m = 1,\ y_0 = 0.2$ and $\tau = 0.01$

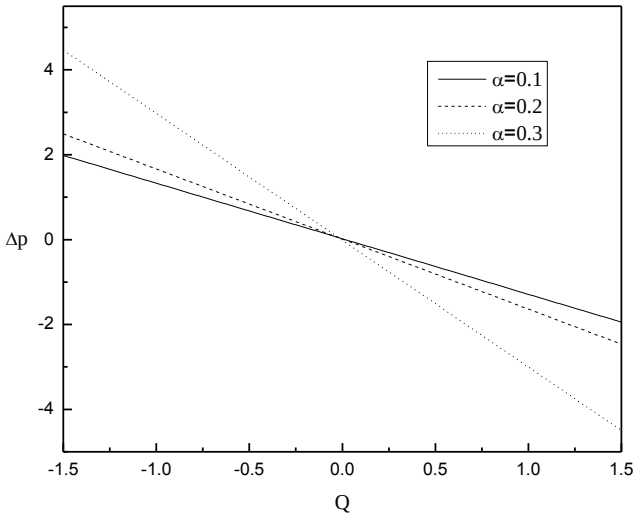

Fig.9. The variation of pressure rise with time-averaged flux for different values α for

$\varphi = 0.6,\ M = 2,\ Da = 0.01,\ m = 1,\ y_0 = 0.2$ and $\tau = 0.01$

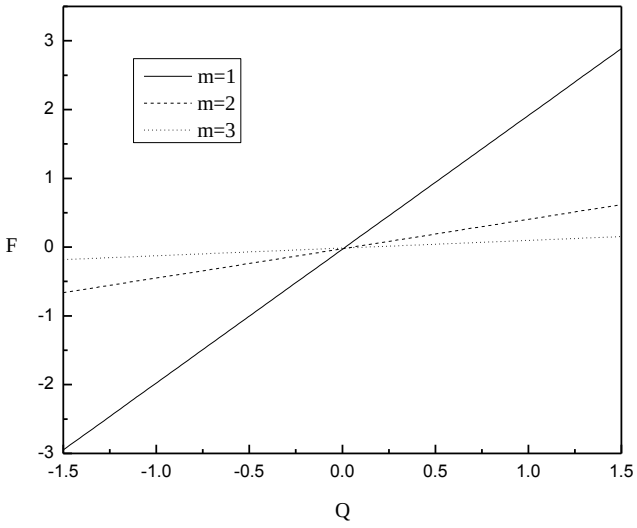

Fig.10. The variation of frictional force with time-averaged flux for different values of m for $\varphi = 0.6,\ M = 2,\ \mathrm{Da} = 0.01,\ \alpha = 0.1,\ y_0 = 0.2$ and $\tau = 0.01$

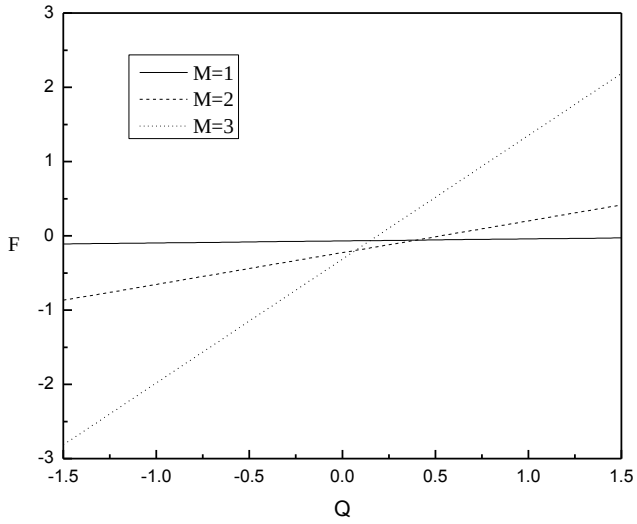

Fig. 11. The variation of frictional force with time-averaged flux for different values of M for $\varphi = 0.6,\ m = 2,\ \mathrm{Da} = 0.01,\ \alpha = 0.1,\ y_0 = 0.2$ and $\tau = 0.1$

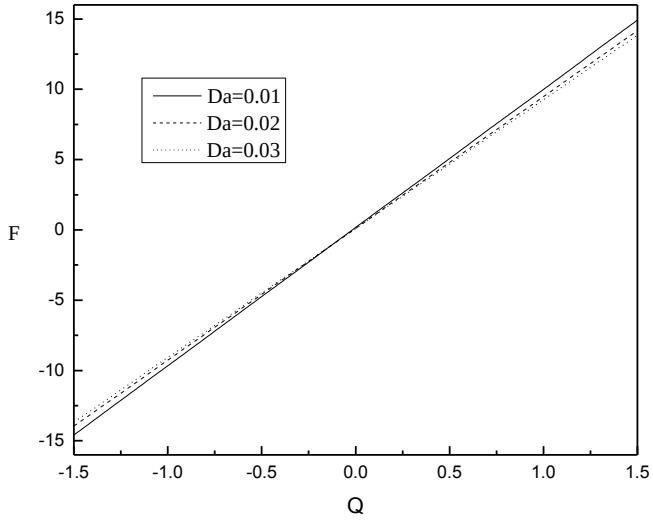

Fig. 12. The variation of frictional force with time-averaged flux for different values of

Da **for** $\varphi = 0.6,\ m = 1,\ M = 4,\ \alpha = 0.1,\ y_0 = 0.2$ and $\tau = 0.01$

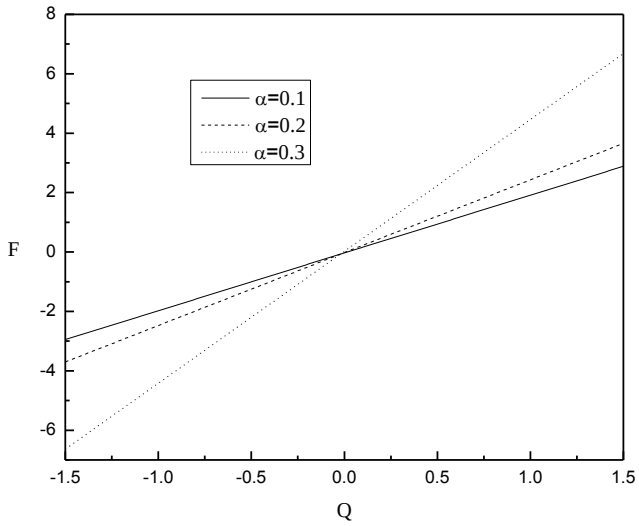

Fig. 13. The variation of frictional force with time-averaged flux for different values of α **for**

$\varphi = 0.6,\ m = 1,\ M = 2,\ Da = 0.01,\ y_0 = 0.2$ and $\tau = 0.01$

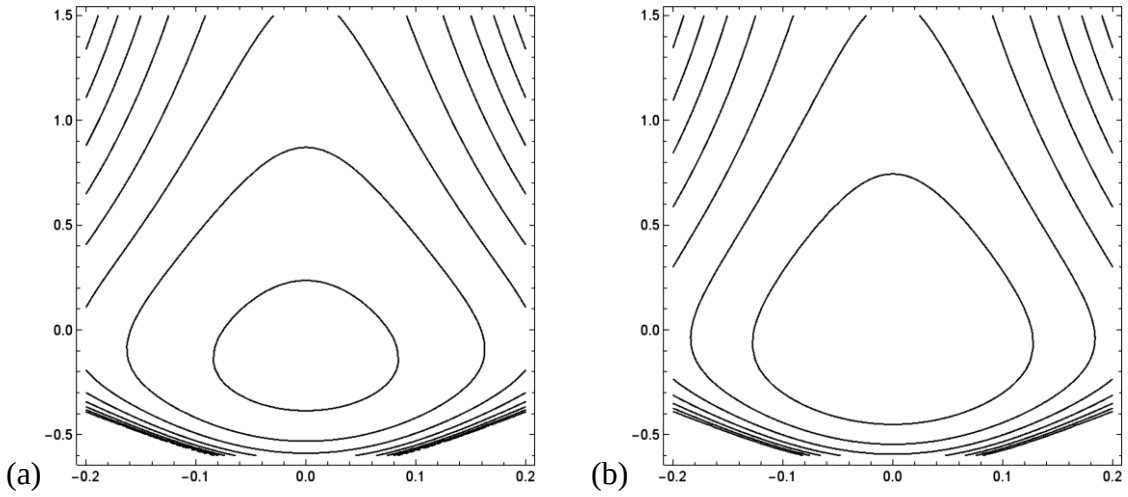

Fig. 14. Streamlines for different values of m: (a) $m = 1$, (b) $m = 1.1$. The other parameters chosen are $\varphi = 0.6$, $Da = 0.1$, $\alpha = 0.1$, $M = 2$, $y_0 = 0.01$, $Q = 2$ and $\tau_0 = 0.01$

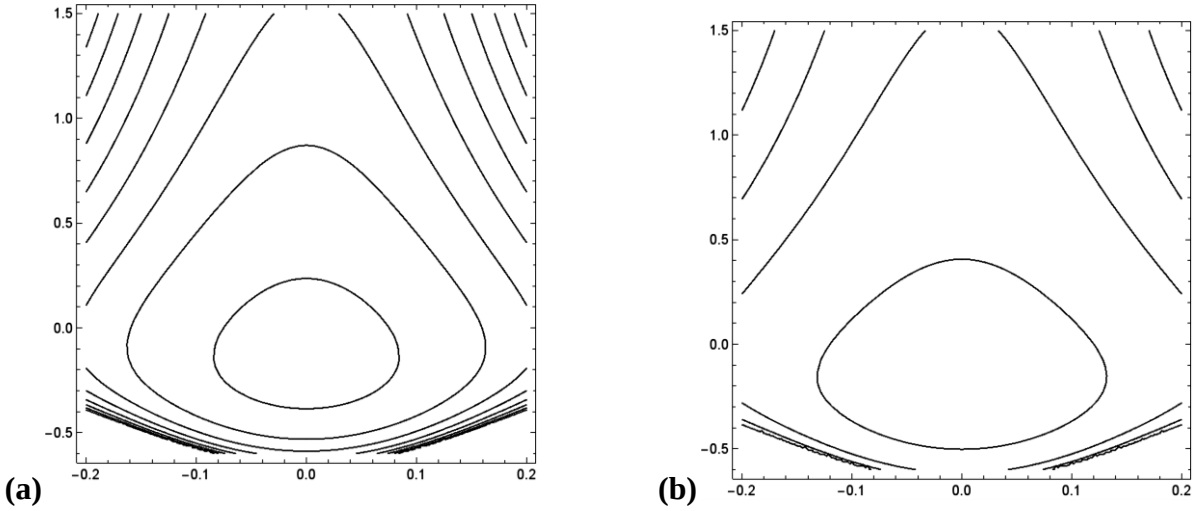

Fig. 15. Streamlines for different values of M: (a) $M = 2$, (b) $M = 2.1$. The other parameters chosen are $\varphi = 0.6$, $Da = 0.1$, $\alpha = 0.1$, $m = 1$, $y_0 = 0.1$, $Q = 2$ and $\tau_0 = 0.01$

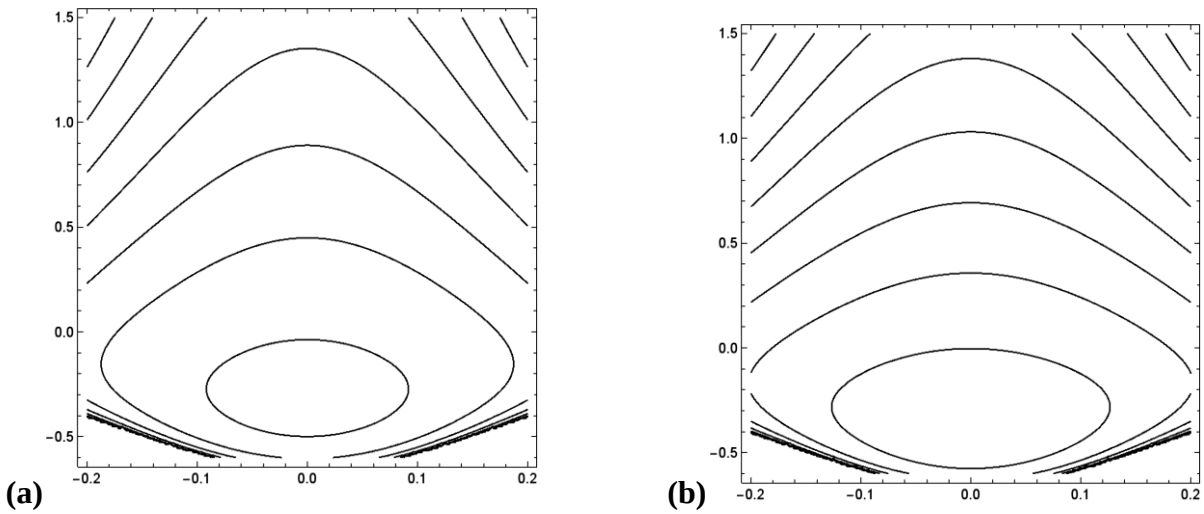

Fig. 16. Streamlines for different values of Q : (a) $Q = 2.5$, (b) $Q = 3$. The other parameters chosen are $\varphi = 0.6$, $Da = 0.1$, $\alpha = 0.1$, $m = 1$, $y_0 = 0.1$, $M = 2$ and $\tau_0 = 0.01$

REFERENCES

1. Latham TW. Fluid motion in a peristaltic pump. M.S. Thesis, MIT, Cambridge, MA. 1966.
2. Fung YC and Yih CS. Peristaltic transport. Journal of Applied Mechanics. 1968; 35: 669-75. Abbasi FM, Maimoona SA and Shehzad Gul. Hall effects on peristalsis of boron nitride-ethylene glycol nanofluid with temperature dependent thermal conductivity. Physica E: Low-dimensional Systems and Nanostructures. 2018; 99: 275-284.
3. Shapiro AH, Jaffrin MY and Weinberg SL. Peristaltic pumping with long wave-length at low Reynolds number. Journal of Fluid Mechanics. 1969; 37: 799-825.
4. Brasseur JG, Corrsin S and NAN Q LU. The influence of a peripheral layer of different viscosity on peristaltic pumping with Newtonian fluids. Journal of fluid Mechanics. 1987; 174: 495-519.
5. Bugliarello G and Sevilla J. Velocity distribution and other characteristics of steady and pulsatile blood flow in fine glass tubes. Journal of Biorheology. 1970; 7:85-107.
6. Cockelet GR. The rheology of human blood. Journal of Biomechanics (Prentice Hall. Englewood cliffs. N. J.). 1972; 63- 103.
7. Srivastava LM and Srivastava VP. Peristaltic transport of blood: Casson model II. Journal of Biomechanics. 1984; 17: 821-829.
8. Comparini E and Mannucci P. Flow of a Bingham fluid in contact with a Newtonian fluid in a channel. Journal of Mathematical Analysis and Applications. 1998; 227 (2): 359-81.

9. Dharmendra T, Ashu Yadav O and Anwar Beg. Electro-Kinetically driven peristaltic transport of viscoelastic physiological fluids through a finite length capillary: Mathematical modeling. Mathematical biosciences. 2017; 283: 155-168.
10. Vajravelu K, Sreenadh S, Devaki P and Prasad KV. peristaltic pumping of a Casson fluid in an elastic tube. Journal of Applied Fluid Mechanics. 2016; 9(4): 1897-1905.
11. Rathod VP and Laxmi Devindrappa. Effects of heat transfer on the peristaltic MHD flow of a Bingham fluid through a porous medium in a channel. Int. J.Biomathematics. 2014; 7:1450060-20.
12. Hayat T, Ali N and Asghar S. Hall effects on peristaltic flow of a Maxwell fluid in a porous medium. Physics Letters A. 2007; 363 (5):397–403.
13. Asghar S, Mohyuddin MR and Hayat T. Effects of hall current and heat transfer on flow due to a pull of eccentric rotating disks. International Journal of Heat and Mass Transfer. 2005; 48(3-4): 599–607.
14. Gad NS. Effect of Hall currents on interaction of pulsatile and peristaltic transport induced flows of a particle-fluid suspension. Applied Mathematics and Computation. 2011; 217(9): 4313–4320.
15. Hussain Q, Hayat T, Asghar S and Alsaadi F. Heat and mass transfer analysis in variable viscosity peristaltic flow with Hall current and ion slip. Journal of Mechanics in Medicine and Biology. 2016; 16(4): 1650047-73.
16. Ellahi R, Bhatti MM and Pop I. Effects of hall and ion slip on MHD peristaltic flow of Jeffrey fluid in a non-uniform rectangular duct. International Journal of Numerical Methods for Heat and Fluid flow. 2016; 26: 1802-20.
17. Abbasi FM, Maimoona Gul SA and Shehzad. Hall effects on peristalsis of boron nitride-ethylene glycol nanofluid with temperature dependent thermal conductivity. Physica E: Low-dimensional Systems and Nanostructures. 2018; 99: 275-284.